Structure
Article

Metal Ion Roles and the Movement of Hydrogen during Reaction Catalyzed by D-Xylose Isomerase: A Joint X-Ray and Neutron Diffraction Study

Andrey Y. Kovalevsky,[1,*] Leif Hanson,[2] S. Zoe Fisher,[1] Marat Mustyakimov,[1] Sax A. Mason,[3] V. Trevor Forsyth,[3,4] Matthew P. Blakeley,[3] David. A. Keen,[5] Trixie Wagner,[1,7] H.L. Carrell,[6] Amy K. Katz,[6] Jenny P. Glusker,[6] and Paul Langan[1,2,*]

[1]Bioscience Division, Los Alamos National Laboratory, MS M888, Los Alamos, NM 87545, USA
[2]Chemistry Department, University of Toledo, Toledo, OH 43606, USA
[3]Institut Laue Langevin, 6 rue Jules Horowitz, BP 156, 38042 Grenoble Cedex 9, France
[4]EPSAM/ISTM, Keele University, Staffordshire, ST5 5BG, UK
[5]ISIS Facility, Rutherford Appleton Laboratory, Harwell Science and Innovation Campus, Didcot OX11 0QX, Oxon, UK
[6]Fox Chase Cancer Center, 333 Cottman Avenue, Philadelphia, PA 19111, USA
[7]Present address: Novartis Institutes for BioMedical Research, 4002 Basel, Switzerland
*Correspondence: ayk@lanl.gov (A.Y.K.), langan_paul@lanl.gov (P.L.)
DOI 10.1016/j.str.2010.03.011

SUMMARY

Conversion of aldo to keto sugars by the metalloenzyme D-xylose isomerase (XI) is a multistep reaction that involves hydrogen transfer. We have determined the structure of this enzyme by neutron diffraction in order to locate H atoms (or their isotope D). Two studies are presented, one of XI containing cadmium and cyclic D-glucose (before sugar ring opening has occurred), and the other containing nickel and linear D-glucose (after ring opening has occurred but before isomerization). Previously we reported the neutron structures of ligand-free enzyme and enzyme with bound product. The data show that His54 is doubly protonated on the ring N in all four structures. Lys289 is neutral before ring opening and gains a proton after this; the catalytic metal-bound water is deprotonated to hydroxyl during isomerization and O5 is deprotonated. These results lead to new suggestions as to how changes might take place over the course of the reaction.

INTRODUCTION

Enzyme catalysis is often a multistep process that can be understood at a molecular level only through a detailed characterization of each step. Structural information from X-ray crystallographic studies of enzymes in complex with their substrates, cofactors, inhibitors, transition state analogs, and products can be thought of as providing static snapshots of different steps along a reaction pathway and can lead to hypotheses about reaction mechanisms. The enzyme D-xylose isomerase (XI) (EC 5.3.1.5) is a crucial enzyme in sugar metabolism, with important commercial applications, notably in the production of biofuels and soft-drink sweeteners (Bhosale et al., 1996; Hartley et al., 2000; Chandrakant and Bisaria, 2000a, 2000b). It binds two divalent metal cations and catalyzes the interconversion of the aldo sugars D-xylose and D-glucose to the keto sugars D-xylulose and D-fructose, respectively. The reaction (Figure 1) is a multistep process and is thought to involve hydrogen (H) transfer in at least two of the stages (Asboth and Naray-Szabo, 2000).

XI from *Streptomyces rubiginosus* is a tetramer of identical subunits, each with a $(\alpha/\beta)_8$ barrel fold and an active site located at the C terminus of the β-barrel. Magnesium is the physiological metal found at two metal binding sites in the active site, M1 and M2, binding directly to water molecules as well as to active-site residues. M1 binds Glu181, Glu217, Asp245, Asp287, and two water molecules (W2 and W3); M2 binds Glu217 (shared with M1), His220, Asp255 (bidentate), Asp257, and the catalytic water D_2O^{cat}. It is found that M2 has a more distorted octahedral coordination polyhedron than does M1 (see Figure 2).

Since we first determined the structure of XI (Carrell et al., 1989), many crystal structures relevant to its reaction mechanism have been studied extensively by X-ray crystallography (Fenn et al., 2004). Several mechanisms consistent with these data have been proposed (Carrell et al., 1989; Fenn et al., 2004; Rose et al., 1969; Collyer et al., 1990; Whitlow et al., 1991; Allen et al., 1994a). They differ in the exact location and mode of transfer of H at each step. Unfortunately, one limitation of X-ray studies is the inability to determine the location of H atoms; labile H atom positions proved difficult to locate in XI even at the ultra-high resolution of 0.9 Å (Katz et al., 2006). Neutron diffraction studies, on the other hand, can provide H locations, especially if hydrogen is replaced by its isotope deuterium. Transferable hydrogen (attached to N or O) can be replaced by deuterium by soaking the enzyme in D_2O. Alternatively, a perdeuterated molecule may be synthesized. We present here the crystal structures of two complexes of XI determined by neutron protein crystallography and representative of two stages in the reaction catalyzed by this enzyme.

Our neutron crystallographic studies of *Streptomyces rubiginosus* XI were initiated by the 1.8 Å neutron diffraction study (denoted by _n in the name) of the structure of the binary complex of the native enzyme with Co^{2+}, designated XI-Co_n (PDB ID: 2GVE) (Katz et al., 2006). Our aim was to address the

 ©2010 Elsevier Ltd All rights reserved

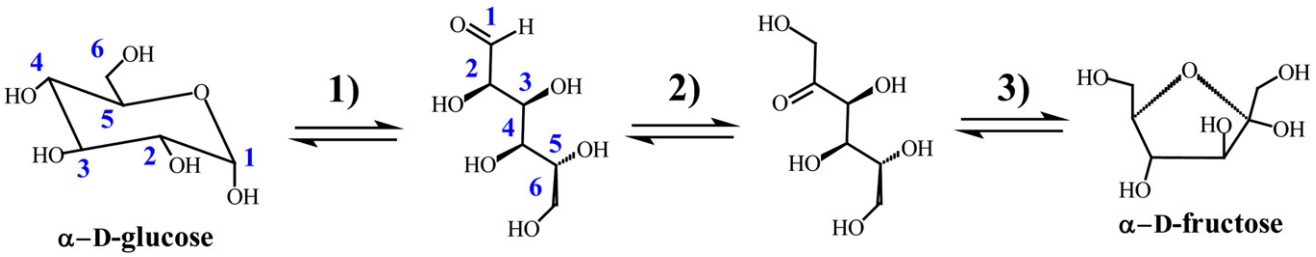

Figure 1. D-Glucose-to-D-Fructose Interconversion Reaction
The reaction catalyzed by XI has been represented as consisting of three major steps: (1) ring opening, (2) isomerization, and (3) ring closure.

problem of locating H atoms by way of deuterated species. Subsequently, we determined the 2.2 Å neutron structure of the ternary complex of the native enzyme with Mg^{2+} and D-xylulose; D-xylose (that had been introduced as substrate) had been catalytically converted to its reaction product D-xylulose. This structure was designated XI-Mg-Product_n (PDB ID: 3CWH) (Kovalevsky et al., 2008). These two published structures (2GVE with metal and 3CWH with both metal and product) revealed some unexpected results and insights into the reaction mechanism that could not have been provided by X-ray crystallography. In these structure determinations, the power of neutron crystallography in determining H (as D or H) atom locations, and possible movements of the atoms during the reaction, was demonstrated. In particular, while Lys289 is neutral and D_2O^{cat} is a water molecule in XI-Co_n, in XI-Mg-Product_n Lys289 is protonated (positively charged) and D_2O^{cat} has become activated to a hydroxyl anion (that lies in the proximity of the isomerization location near C1 and C2). However, the information from these two structures (2GVE and 3CWH) was insufficient for us to be able to infer the complete transfer of hydrogen during the catalyzed reaction, and suggested the need for further neutron studies.

We present here two new neutron diffraction studies. These involve the ternary complex of the enzyme with Cd^{2+} and D-glucose substrate (bound in its cyclic form) (PDB ID: 3KCL) and the ternary complex of the enzyme with Ni^{2+} and D-glucose substrate (bound in its linear form) (PDB ID: 3KCO). These are designated XI-Cd-CyclicSugar_n and XI-Ni-LinearSugar_n, respectively. These two new neutron structures, along with the two neutron structures previously reported by us (XI-Co_n and XI-Mg-Product_n), represent different stages of the reaction catalyzed by XI. Four neutron structures are discussed here:

1. XI-Co_n, no ligand (2GVE [published]) (Katz et al., 2006).
2. XI-Cd-CyclicSugar_n, bound cyclic sugar, before ring opening (3KCL [this work]).
3. XI-Ni-LinearSugar_n, bound linear substrate after ring opening and before isomerization (3KCO [this work]).
4. XI-Mg-Product_n, bound linear product after isomerization (3CWH [published]) (Kovalevsky et al., 2008).

A detailed characterization and comparison of each of these four neutron structures will be presented here. They provide direct information on the ionization states of the side chains and ligands, and the coordination of metal ions in the enzyme. They lead to suggestions as to how changes might take place over the course of the reaction and provide new insights into the overall reaction mechanism of XI.

Our selection of the two ternary complexes for neutron studies resulted from a search for different metal cofactors that would allow sugar binding in the active site but would inhibit the catalytic reaction either before or after the ring-opening step. XI has an absolute requirement for two divalent metal cations, designated M1 (at the structural metal site) and M2 (at the catalytic metal site) (Whitlow et al., 1991) to be fully active (Chen, 1980; Callens et al., 1986). It has been reported that metal cations that have ionic radii $\leq$ 0.8 Å, such as Mg^{2+},

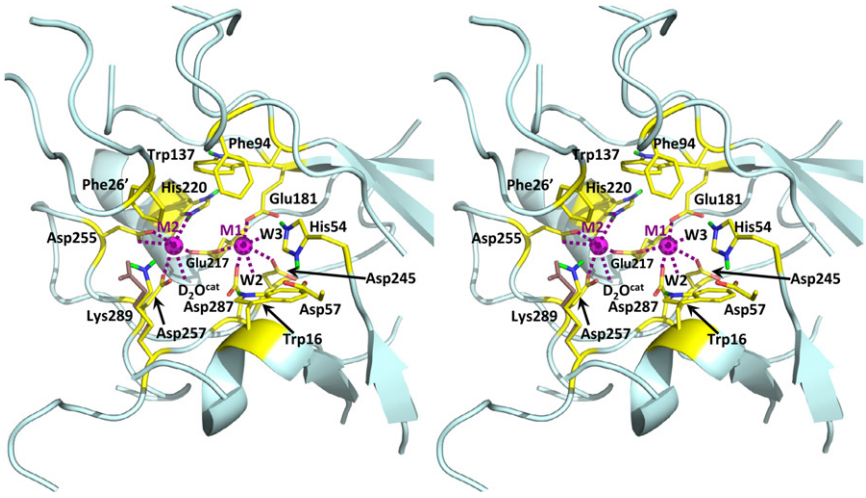

Figure 2. Active Site of Native XI in XI-Co_n
The residues coordinating metal cofactors, represented as magenta spheres, and those lining the cavity, Trp16, His54, Phe94, Trp137, and Phe26′, are shown. Phe26′ belongs to a symmetry-related subunit.

Mn^{2+}, Co^{2+}, and Fe^{2+}, activate XI, while larger alkali-earth metal cations Ca^{2+}, Ba^{2+}, and Sr^{2+}, and transition metal cations Hg^{2+}, Pb^{2+}, Ni^{2+}, Cu^{2+}, and Cd^{2+} inhibit XI (Chen, 1980; Danno, 1970). Trivalent metal cations Al^{3+} and Fe^{3+} reduce the activity of XI (Suekane et al., 1978). M2 has a high affinity for Mn^{2+}, Co^{2+}, Cd^{2+}, and Pb^{2+}, whereas M1 preferentially binds Mg^{2+}, Al^{3+}, and larger lanthanides (Collyer et al., 1990; Henrick et al., 1989). In our initial attempts to change metal cofactors by dialysis against the metal of choice, we found that Mg^{2+} was often retained at the M1 position, with a variety of metal ions of choice occupying the M2 position. In summary, from these findings it appears that the structural metal site, M1, prefers to bind Mg^{2+}, Mn^{2+}, or Co^{2+}, while the catalytic metal site, M2, will bind a fairly wide range of divalent metal ions, although many may inhibit the enzyme. In order to be able to obtain a completely metal-free (*apo*) enzyme (so that we could add Ni^{2+} or Cd^{2+}), we adopted the protocol for rigorous and repeated dialysis against EDTA that is described later in the Experimental Procedures.

Structural Studies

In readiness for neutron studies, we determined several X-ray structures (denoted by _x in the name) of XI complexes. The following were studied in this work: the X-ray structures of XI-Mg/Ni_x to 1.6 Å resolution (PDB ID: 3KBW), XI-Ni_x to 1.8 Å resolution (PDB ID: 3KBV), XI-Cd_x to 1.8 Å resolution (PDB ID: 3KBS), XI-Cd-CyclicSugar_x to 2.0 Å resolution (PDB ID: 3KBM), and XI-Ni-LinearSugar_x to 1.53 Å resolution (PDB ID: 3KBN). The X-ray structures of XI-Cd-CyclicSugar_x and XI-Ni-LinearSugar_x were used as starting points for the refinement of the corresponding neutron structures. In this work, we therefore present two new neutron and five new X-ray crystallographic structures, all determined at room temperature.

For the two neutron studies, the enzyme was subjected to hydrogen/deuterium exchange by vapor exchange with D_2O so that accessible and exchangeable H atoms (in water or bound to O or N) were replaced by D. In addition, the ligand D-glucose that was bound to the enzyme was perdeuterated (all H replaced by D during organic synthesis). The great advantage of neutron crystallography is that D atoms appear as strong positive peaks in neutron scattering density maps, thereby revealing the locations of isotopically exchanged H atoms, while H atoms (neutron scattering length -3.74×10^{-15} m) appear as negative troughs (and therefore can be distinguished from D). Both C and O (neutron scattering lengths 6.65 and 5.80×10^{-15} m, respectively) scatter about the same as D (6.67×10^{-15} m), while N (9.36×10^{-15} m) scatters more. The values for the metal ions that will be described are: Mg^{2+}, 5.38×10^{-15} m; Mn^{2+}, -3.73×10^{-15} m; Co^{2+}, 2.49×10^{-15} m; Cd^{2+}, 4.87×10^{-15} m; and Ni^{2+}, 10.3×10^{-15} m (Sears, 1992). Note in these that Mn^{2+} gives a negative peak, and therefore, if present with Mg^{2+}, will reduce the metal ion peak height. The advantages and limitations associated with neutron crystallography have been discussed in a review of recently determined neutron structures (Blakeley et al., 2008).

The crystal structures of XI-Cd-CyclicSugar_n and XI-Ni-LinearSugar_n were determined using a generalized X-ray and neutron (XN) crystallographic analysis approach that exploits the complementarities of X-ray and neutron data, and provides more complete (including H) and more accurate overall structures (Adams et al., 2009). The resolutions of the X-ray and neutron data sets that were used to jointly refine the structures were 2.0 Å and 2.0 Å for XI-Cd-CyclicSugar_x and XI-Cd-CyclicSugar_n, and 1.5 Å and 1.8 Å for XI-Ni-LinearSugar_x and XI-Ni-LinearSugar_n, respectively. We were able to carry out these lengthy experimental neutron diffraction procedures by obtaining large crystals and by the use of two neutron protein crystallography beam lines, one at the PCS at LANSCE and the other, D19, Institut Laue Langevin.

Our key findings are that during ring opening of the cyclic sugar, H is moved to Lys289, which is neutral before ring opening. O5 is deprotonated after ring opening. His54 remains doubly protonated on its ring N's in all four structures and appears to play a significant role, as does the metal ion, in ring opening. During isomerization the metal ion moves toward the aldehyde terminus of the linear sugar to bind to O1 and O2. H is removed from the metal-bound catalytic water (so that it becomes a hydroxyl ion). C2 and O2 also lose H, and O1 and C1 gain H. These results lead to new suggestions as to how changes might take place over the course of the reaction.

RESULTS

The neutron data obtained for the XI complexes are summarized in Table 1, and for the corresponding X-ray data are given in Table 2 and Table S2 (available online). Results for the different stages of the enzyme-catalyzed reaction represented by XI-Co_n, XI-Cd-CyclicSugar_n, XI-Ni-LinearSugar_n, and XI-Mg-Product_n for the four neutron studies are summarized in Table 3, which also contains a list of the changes in metal ligation, the protonation state, and the hydrogen bonding of key amino acid side-chains and the catalytic water. We present descriptions of the active sites of XI-Cd-CyclicSugar_n and XI-Ni-LinearSugar_n, and point out important differences between them and the active sites of the previously studied XI-Co_n and XI-Mg-Product_n (Figure S1).

XI-Cd-CyclicSugar_n

In XI-Cd-CyclicSugar_n, the cyclic form of perdeuterated D-glucose with all H replaced by D, coordinates to M1. The D atoms of the O3 and O4 hydroxyl groups of the D-glucose then form strong hydrogen bonds to the catalytic water molecule and Oε2 of Glu181, respectively (with O…O distances of 2.6 Å and 2.5 Å). Four water molecules, W2, W3, W5, and W6, are displaced from the active site area of XI-Co_n (see Figures 3A–3C). These water molecules lie between M1 and His54 in XI-Co_n. Water molecules, W2, W3, and W5 in XI-Co_n, are replaced by glucose oxygen atoms (O3, O4, and O5, respectively). The O5 of glucose takes the place of W5 and accepts a D in a hydrogen bond (with O…N distance of 2.8 Å) with Nε2 of His54. In the ligand-free enzyme the atom Nε2 of His54 donates a D to W5 in an N-H…O hydrogen bond (with O…N distance of 2.9 Å). The position of W6 in XI-Cd-CyclicSugar_n is taken by the C2-C3 bond of the cyclic substrate.

There are many similarities between the ligand-free enzyme (XI-Co_n) and the enzyme with a bound cyclic substrate (XI-Cd-CyclicSugar_n). In both structures D_2O^{cat} and W4 remain in the active site near M2. In XI-Cd-CyclicSugar_n, Lys183 remains

Table 1. Room Temperature Neutron Crystallographic Data Collection and Refinement Statistics

Enzyme Complex	XI-Cd-CyclicSugar_n	XI-Ni-LinearSugar_n
Data collection		
Wavelength, Å	2.422	0.7 – 6.5
Resolution	51.5 – 2.0 (2.1 – 2.0)	40.5– 1.8 (1.9 – 1.8)
No. reflections measured	67807 (5578)	140375 (9310)
No. unique reflections	29062 (3386)	37568 (4655)
Data rejection criteria	no observations & $\|F\| = 0$	no observations & $I < 1.5\sigma(I)$
Redundancy	2.3 (1.6)	3.2 (1.9)
$<I/\sigma(I)>$	6.3 (1.8)	4.0 (1.5)
Completeness	89.0 (76.4)	84.4 (72.5)
R_{sym}[a]	0.175(0.344)	0.236 (0.359)
Joint X-N Refinement[b]		
Resolution range, Å	20 – 2.00 / 20 – 2.00	20 – 1.80 / 20 – 1.53
R_{work}[c]	0.188 / 0.173	0.274 / 0.199
R_{free}[d]	0.211 / 0.194	0.294 / 0.211
No. protein atoms including H and D	5983	5987
No. D_2O molecules	199	309
Rmsd bond lengths, Å	0.012	0.008
Rmsd bond angles, °	1.454	1.011
Average B factors, Å^2		
Main chain	21.9	17.7
Side chain	24.4	20.1
Solvent	35.4	33.7
D-[d_{12}]-glucose	24.5	25.8

[a] $R_{sym} = \Sigma \mid I - <I> \mid / \Sigma <I>$.
[b] Values separated by forward slashes are for the refinement on neutron data and X-ray data, respectively.
[c] $R_{work} = \Sigma \mid F_O - F_C \mid / \Sigma \mid F_O \mid$.
[d] R_{free} is calculated in the same way as R_{work} for data omitted from refinement (5% of reflections for all data sets).

Table 2. Room Temperature X-Ray Crystallographic Data Collection and Refinement Statistics

Enzyme Complex	XI-Cd-CyclicSugar_x	XI-Ni-LinearSugar_x
Data collection		
Wavelength, Å	1.5418 (Cu Kα)	1.5418 (Cu Kα)
Space group	I222	I222
Unit cell dimensions a, b, c (Å)	a = 94.20 b = 99.43 c = 102.99	a = 94.00 b = 99.67 c = 102.86
Resolution, Å	20.00–2.00 (2.07–2.00)	24.07–1.53 (1.58–1.53)
No. reflns. measrd.	112052	248216
Unique reflns	30084 (2971)	72287 (6037)
Redundancy	3.72 (3.6)	3.43 (2.79)
Completeness, %	91.2 (93.3)	99.2 (93.5)
$<I/\sigma(I)>$	8.8 (3.5)	8.7 (2.2)
R_{sym}[a]	0.100 (0.285)	0.067 (0.375)
Refinement		
Resolution range, Å	20 – 2.00	20 – 1.53
R_{work}[b]	0.176	0.138
R_{free}[c]	0.211	0.182
No. solvent molecules	210	341
Rmsd bond lengths (Å)	0.006	0.012
Rmsd bond angles, °	0.022	0.028
Average B factors, Å^2		
Main chain	28.3	24.0
Side chain	34.9	30.8
Solvent	37.6	41.1
D-[d_{12}]-glucose	37.8	36.5

[a] $R_{sym} = \Sigma \mid I - <I> \mid / \Sigma <I>$.
[b] $R_{work} = \Sigma \mid F_O - F_C \mid / \Sigma \mid F_O \mid$.
[c] R_{free} is calculated in the same way as R_{work} for data omitted from refinement (5% of reflections for all data sets).

hydrogen-bonded to W4 and Lys289 remains neutral and rotated away from Asp257 and Asp287, as in XI-Co_n. There are slight differences in the positions of active-site carboxylic groups and D_2O^{cat} between XI-Co_n and XI-Cd-CyclicSugar_n, with a mean shift of ~0.5 Å possibly to accommodate the larger cation (Cd2+ ionic radius 0.95 Å, Co^{2+} ionic radius 0.65 Å). The ring of His54 is doubly N-protonated in all of the neutron structures that we have determined, including in XI-Cd-CyclicSugar_n.

The binding of His220 to M2 with a distance of 2.7 Å is interesting. The mean Co-N(imidazole) distance in structures in the PDB determined at near atomic resolution has been reported to be 2.04(9) Å (Harding, 2006). According to a recently used definition, coordination of a donor to Co requires the atom of the donor being within 2.79 Å of the metal (Harding, 2001). His220, therefore, only just makes the criterion for coordination to M2 and must be quite weakly bound. The coordinating atom Nε2 is found to be protonated 50% of the time in XI-Co_n. This suggests that His220 tends to break its coordination to M2.

It appears that both the size of the metal cation and the presence of the sugar are responsible for any subtle differences between the active sites of the neutron crystallographic structures of XI-Co_n and XI-Cd-CyclicSugar_n. This follows from an X-ray crystallographic structure of XI complexed with the large cation Cd^{2+} but with no substrate present (PDB ID: 3KBS, designated XI-Cd_x). Metal ion size difference is indicated by a root-mean-square deviation of 0.6 Å for XI-Cd_x versus XI-Co_n. The result of ligand binding is a root-mean-square deviation of 0.5 Å for XI-Cd_x versus XI-Cd-CyclicSugar_n. These differences are probably of low significance given that errors in distances for 1.8-2.0 Å resolution structures are normally in the range of 0.2-0.3 Å.

XI-Ni-LinearSugar_n

The Ni^{2+} metal cation in the vicinity of M2 in both XI-Ni-LinearSugar_n and XI-Ni-LinearSugar_x appears to populate two distinct positions, which we designate M2a and M2b, separated by 1.9 Å and with approximately 50/50 occupancies (see Figures 4A–4C). Position M2a is analogous to the M2 location in XI-Co_n, XI-Cd-CyclicSugar_n, and XI-Mg-Product_n, but position M2b is much closer to the linear substrate. The peaks at

Table 3. Chemical Nature, Protonation States, and Metal Ion Coordination in the Four Neutron-Diffraction Structures

	XI-Metal 2GVE (Co2+)	XI-Metal-CyclicSugar This paper	XI-Metal-LinearSugar This paper	XI-Metal-LinearProduct 3CWH (Mg2+)
Protonation states or nature				
His54	+1	+1	+1	+1
Lys183	+1	+1	+1	+1
His220	0/+1 (50/50)	0	0	0
Lys289	0	0	+1	+1
Watercat	D_2O	D_2O	D_2O	OD^-
O1	N/A	–OD	=O (aldehyde)	–OD
O2	N/A	–OD	–OD	O (ketone)
O3	N/A	–OD	–OD	–OD
O4	N/A	–OD	–OD	–OD
O5	N/A	–O– (cyclic)	$–O^-$	$–O^-$
Metal coordination				
M1	E181 E217 D245 D287 W2 W3	E181 E217 D245 D287 O3 O4	E181 E217, D245 D287 O2 O4	E181 E217 D245 D287 O2 O4
M2 or M2a	E217 H220, D255 (chelate) D257 D_2O^{cat}	E217 H220 D255 (chelate) D257 D_2O^{cat}	E217 H220, D255 (chelate) D257 D_2O^{cat}	E217 H220 D255 (chelate) D257 OD^-
M2b			E217 H220 O1 O2 D_2O^{cat}	

M2a and M2b in F_O-F_C omit maps have heights of 52σ and 45σ in electron density and 9σ and 5σ in neutron scattering density, respectively. In the structure with metal ion-bound product (3CWH), there is no disorder in either metal ion position. A second conformation is observed for Asp255, rotated away from the M2a and M2b positions, presumably due to Asp255 losing its coordination with Ni^{2+} when the cation has moved to the M2b position. However, we see no other indication of different coordination arrangements for donors to the metal when it is at the M2a and M2b positions.

In order to investigate if the incidence of two metal subsites is due to the type of metal cation present or to the presence of the linear form of the substrate itself, we determined the X-ray crystallographic structure of XI complexed with Ni^{2+} metal cations, but with no substrate present (PDB ID: 3KBV), designated XI-Ni_x. Ni^{2+} cations were found located only at the M1 and M2 (that is, M2a) positions in this structure. The metal disorder (where M2a may move to M2b) therefore appears to occur as a result of the binding of the linear form of the sugar substrate in the binding site. This experimental suggestion of a movement of the metal ion to facilitate isomerization of the substrate in its linear form is of interest.

In XI-Ni-LinearSugar_n, O1 of linear D-glucose coordinates to the metal cation located at M2b at a distance of 2.3 Å and accepts a hydrogen bond from Lys183 (Figure 4B). Both neutron and X-ray scattering densities clearly show that the C1-O1 group of the bound ligand is an aldehyde, because the O1-C1(D)-C2 group is observed in the $2F_O$-F_C nuclear density map to have a planar configuration. This means that the isomerization step has not taken place in this Ni-containing structure. O1 of D-glucose displaces W4, which mediates the interaction between Lys183 and the O2 hydroxyl of the cyclic substrate in XI-Cd-CyclicSugar_n, as described earlier. The O4 hydroxyl group of D-glucose is in the same location in XI-Ni-LinearSugar_n and XI-Cd-CyclicSugar_n, coordinated to M1. There is a 60° rotation difference about the C3-C4 bond between the cyclic and linear forms of the bound substrate. In XI-Ni-LinearSugar_n, this rotation causes O3 to lose the coordination it had with M1 in XI-Cd-CyclicSugar_n, but allows it to donate a hydrogen in a hydrogen bond to a water molecule that then accepts a hydrogen in a hydrogen bond from Lys289. O3 occupies a position close to the hydrophobic surface of Trp16, which is similar to the position of W6 in XI-Co_n. The O2 hydroxyl, which was positioned in a void between Trp16 and Phe26′ of the symmetry-related subunit in XI-Cd-CyclicSugar_n, is rotated to bind to M1 and M2b in XI-Ni-LinearSugar_n (Figure S2).

The O5 hydroxyl group of the linear glucose is deprotonated in XI-Ni-LinearSugar_n, and therefore is negatively charged. It accepts a D in a strong charge-assisted hydrogen bond with protonated Nε2 of His54 (with O…N distance of 2.6 Å). Interestingly, this is the second time that we have observed this deprotonation as O5 is also negatively charged in XI-Mg-Product_n and remains bound to protonated His54 (with O…N distance of 3.1 Å). In both XI-Cd-CyclicSugar_n and XI-Ni-LinearSugar_n the terminal substituents -CD_2-OD comprising sugar atoms C6 and O6 are well defined by neutron scattering density but poorly defined by electron density (Figure 4C). In XI-Ni-LinearSugar_n, the hydroxymethylene substituent is rotated by about 120° relative to its position in XI-Cd-CyclicSugar_n and forms an O-D…π interaction with Trp16 (Figure S3).

Whereas the side-chain of Lys289 is neutral (ND_2) in XI-Co_n and XI-Cd-CyclicSugar_n, it has gained a proton and is charged (ND_3+) in XI-Ni-LinearSugar_n. The ND_3+ group of Lys289 is also hydrogen bonded to the side chain of Asp257. D_2O^{cat} is D_2O in both XI-Ni-LinearSugar_n and XI-Cd-CyclicSugar_n and occupies the same position.

The linear sugar in XI-Ni-LinearSugar_n superimposes well on the linear product in XI-Mg-Product_n, although it is longer by its CD_2-OD substituent at C5 (Figure 5). In both XI-Mg-Product_n and XI-Ni-LinearSugar_n, the O2 carbonyl and O4 hydroxyl groups are coordinated to M1. In going from XI-Ni-LinearSugar_n to XI-Mg-Product_n, O1 becomes protonated and is a hydroxyl group, while C1 is converted to a methylene substituent CD_2. O1 retains its hydrogen bond to the protonated Lys183 in XI-Mg-Product_n without significant change in distance. The methylene CD_2 group of the linear product xylulose is larger than the aldehyde methyne CD group of the linear substrate glucose, thus forcing the side chain of Phe26′ to move away from its position in XI-Ni-LinearSugar_n. The position and

 ©2010 Elsevier Ltd All rights reserved

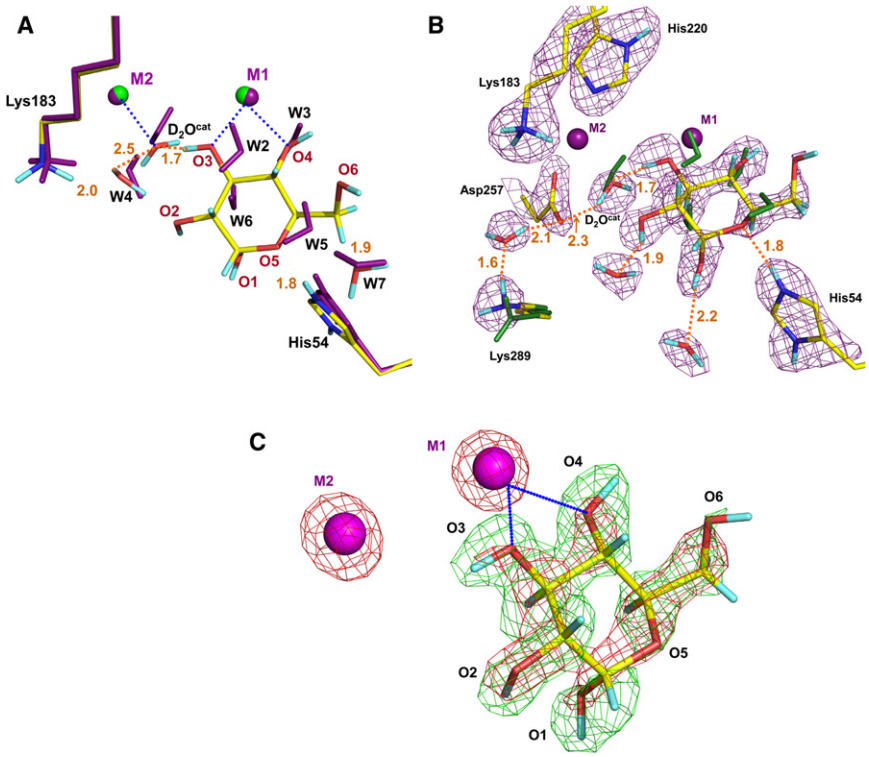

Figure 3. Cyclic Glucose Substrate Binding in XI-Cd_CyclicSugar_n and Comparison with XI-Co_n

Metal coordination to D_2O^{cat} and cyclic glucose is indicated by blue dotted lines; hydrogen bonds are shown as orange dashed lines and the O…D distances are in Å.

(A) Superpositions of water structures in XI-Cd-CyclicSugar_n (colored by atom type) and XI-Co_n (colored magenta) complexes.

(B) Superposition of selected active-site residues and water molecules in XI-Cd-CyclicSugar_n (atom-type colored sticks and violet spheres for Cd(II) cations) and XI-Co_n (dark green sticks). Neutron scattering density shown for XI-Cd-CyclicSugar_n is contoured at 1.6σ level. His54 and Lys183 are protonated, while Lys289 is neutral in both structures. One of the two distinct conformations of Lys289's side chain is shown for XI-Co_n for clarity. Four water molecules are displaced by the cycle of perdeuterated glucose substrate. The catalytic water, marked D_2O^{cat}, retains its position and coordination to M2 in XI-Cd-CyclicSugar_n relative to XI-Co_n.

(C) $2F_O$-F_C neutron scattering (green, contoured at 1.6σ) and electron density (red, contoured at 2σ for light atoms and 10σ for Cd) maps for the cyclic perdeuterated glucose coordinated to Cd cations in XI-Cd-CyclicSugar_n.

hydrogen bonding to Asp257 of Lys289's ND_3^+ group is unchanged in the linear substrate and linear product structures (Figure 6). On the other hand, the catalytic water D_2O^{cat} has clearly lost a proton and has therefore become an OD^- in XI-Mg-Product_n. OD^- has a symmetric bifurcated H-bond with carboxylate of Asp257 (O…O distances of 3.0 Å) and a strong C-H…O contact of 2.6 Å, with the CD_2 methylene group at C1 in xylulose.

DISCUSSION

Sugar Binding

The XI active site in XI-Co_n contains 7 water molecules W2, W3, W4, W5, W6, W7, and D_2O^{cat} (Figure 3A). In XI-Cd-CyclicSugar_n, the O3, O4, and O5 atoms of the substrate occupy the same locations as W2, W3, and W5 in XI-Co_n and, to a certain extent, replace their bonding functionalities. W2, W3, and W5 can be thought of as forming a template for the cyclic substrate to bind to in XI-Co_n. In XI-Ni-LinearSugar_n, the O1 atom occupies the same location as W4. Furthermore, the O2, O3, and O4 atoms occupy the same locations as W2, W6, and W3, respectively. W2, W3, W4, W5, and W6 in XI-Co_n can therefore be thought of as forming a template for the linear substrate.

It has been established that XI is highly stereospecific for the α-pyranose and α-fructofuranose anomers of glucose, xylose, fructose, and xylulose (Asboth and Naray-Szabo, 2000; Schray and Rose, 1971; Bock et al., 1983; Collyer et al., 1992) and that the reactive substrate is the cyclic form of the sugar (Carrell et al., 1989; Collyer et al., 1990; Whitlow et al., 1991; Blow et al., 1992). Site-directed mutagenesis of the residues coordinating the metal cations has provided evidence for the role of M1 in correctly positioning the substrate in the active site (Allen et al., 1994a; Jenkins et al., 1992; Cha et al., 1994). However, in XI-Co_n there is a structured water template for binding both the cyclic and the linear forms of the substrate, suggesting that water structure may play some role in both positioning the cyclic substrate and in facilitating its opening.

Ring Opening

In all four structures, XI-Co_n, XI-Cd-CyclicSugar_n, XI-Ni-LinearSugar_n, and XI-Mg-Product_n, His54 is doubly protonated on N, with the D on Nδ1 hydrogen bonded to the deprotonated carboxylate group of Asp57. The His54-Asp57 pair donates a D in a hydrogen bond to W5 in XI-Co_n. W5 is displaced upon binding of the cyclic sugar in XI-Cd-CyclicSugar_n, with the O5 ring oxygen accepting a D in a hydrogen bond with Nε2 of the His54-Asp57 pair. When the linear substrate is bound in XI-Ni-LinearSugar_n O5 is deprotonated, as in XI-Mg-Product_n, and therefore negatively charged. It also accepts a D in a hydrogen bond with Nε2 of the His54-Asp57 pair. The motif is similar to the Asp-His-Ser motif in the serine proteases (Kossiakoff and Spencer, 1980).

These observations lead to modifications of previous proposals (Collyer et al., 1990; Whitlow et al., 1991; Allen et al., 1994b; Lee et al., 1990; Whitaker et al., 1995) for ring opening that suggest that His54 may act as an acid-base catalyst donating H^+ to the sugar-ring O5 to promote ring opening. In a slightly different mechanism put forward by Fenn, Ringe, and Petsko (Fenn et al., 2004), Asp57 abstracts a proton from a water molecule and passes it over to the Nδ1 atom of His54, already protonated at Nε2. The initially neutral His54 thus becomes charged (doubly protonated) and then functions in concert with the hydroxyl anion produced by Asp57 to donate a proton to

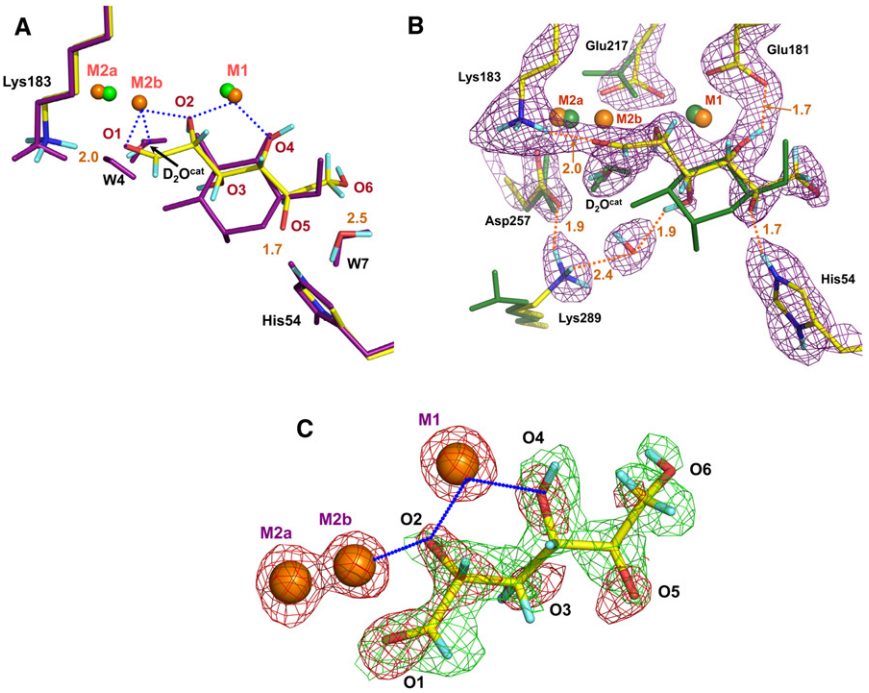

Figure 4. Linear Glucose Substrate Binding in XI-Ni_LinearSugar_n and Comparison with XI-Cd_CyclicSugar_n

Metal coordination to D_2O^{cat} and cyclic glucose is indicated by blue dotted lines; hydrogen bonds are shown as orange dashed lines and the O…D distances are in Å.

(A) Superpositions of substrates and water structures in XI-Ni-LinearSugar_n and XI-Cd-CyclicSugar_n complexes.

(B) Superposition of selected active-site residues and water molecules in XI-Ni-LinearSugar_n (atom-type colored sticks and orange spheres for Ni^{2+} cations) and XI-Cd-CyclicSugar_n (dark green sticks). Neutron scattering density contoured at 1.6σ level is shown for XI-Ni-LinearSugar_n, in which His54, Lys183, and Lys289 are protonated, while Lys289 is neutral and rotated away from Asp257 in XI-Cd-CyclicSugar_n. Carbon atoms C3, C4, C5, and C6 of the linear and cyclic perdeuterated glucose superimpose well, whereas C2 and C1 are rotated toward the catalytic metal M2. M2 has two distinct positions, M2a and M2b 1.9 Å apart, with M2b coordinating O1 and O2 of the linear intermediate. The catalytic water marked D_2O^{cat} retains its position in XI-Ni-LinearSugar_n relative to XI-Cd-CyclicSugar_n.

(C) $2F_O$-F_C neutron scattering (green, contoured at 1.4σ) and electron density (red, contoured at 1.4σ for light atoms and 6σ for Ni) maps for the linear perdeuterated glucose coordinated to Ni cations in XI-Ni-LinearSugar_n.

O5 and to pull one from the O1 hydroxyl. From the experimental evidence presented here, it would appear that doubly protonated His54 does not permanently donate a proton to O5 after the ring opening stage. This is consistent with mutagenesis studies in which it was found that when His54 is substituted by Asn or Gln, whose side-chain amide groups are incapable of binding or donating a proton, only the slowing of the conversion reaction is observed (Lee et al., 1990; Whitaker et al., 1995). The catalytic residue at the position of His54 therefore does not have to be able to donate a proton in order to open the sugar ring. One possibility is that His54 (or Asn, or Gln) may transiently give its extra proton up to O5 and then reclaim it after the C1-O5 endocyclic bond is broken. However, we also note that Lys289 is neutral, ND_2, in XI-Co_n and XI-Cd-CyclicSugar_n before ring opening, and charged, ND_3^+, in XI-Ni-LinearSugar_n and XI-Mg-Product_n after sugar ring opening. This would suggest that Lys289 is gaining a proton during the ring-opening step. One possibility is that Lys289 participates in the ring opening step as a base abstracting H from the O1 hydroxyl. If this is the case, then once the ring is open O1 would swing toward Lys183 and M1, displacing W4, which is conserved in XI-Co_n and XI-Cd-CyclicSugar_n structures (Figures 3A and 4A). W4 acts as mimic for O1 of the linear sugar and protonated Lys183 anchors the latter to its correct position by donating H in a hydrogen bond and preparing the aldehyde group for the isomerization.

Although a role for Lys289 in ring opening is still hypothetical, it may be significant that the sequence alignment of XI from a variety of microbial sources shows that Lys289 is conserved among the species (Bhosale et al., 1996; Hartley et al., 2000; Farber et al., 1989; Lavie et al., 1994), pointing to its importance for XI to function. Although this position is substituted with a histidine in XI from *Thermus thermophilus*, the substitution results in a residue that can still be protonated during the ring-opening step. XI is most active at a pH of ~7.7 and its activity drops substantially below 7.0. The impaired XI activity measured below a pH of 7 could be explained by the protonation of Lys289 and, perhaps, other active-site residues, e.g., His220, which is observed to be only partially protonated in XI-Co_n.

The pH dependence of the specific activity of XI for the catalytic reaction is bell-shaped, with two apparent pKa values of 6.8 and 8.4 (Lee et al., 1990; Gaikwad et al., 1988). The fact that His54 makes direct contact with the ring oxygen of the substrate and is doubly protonated throughout the entire reaction in crystals grown at pH of 7.7 suggests that it could be associated with the higher pKa value. Mutations of His54 to residues incapable of being protonated/deprotonated, such as Asn or Gln, result in enzymes with activities that are pH insensitive in the 5.0-8.5 pH range (Jenkins et al., 1992). The pKa of free histidine in solution is considerably lower than the value of 8.4, and therefore exploring the association of His54, and other amino acid residues, with the kinetic pKa's, will require further neutron crystallographic studies at different values of pH.

Isomerization

In XI-Co_n, XI-Cd-CyclicSugar_n, and XI-Ni-LinearSugar_n, the catalytic water bound to M2 is a D_2O, whereas in XI-Mg-Product_n it is an OD^- hydroxyl anion. This would suggest that the catalytic water molecule donates a proton during the isomerization reaction. Furthermore, during isomerization, which corresponds to going from XI-Ni-LinearSugar_n to XI-Mg-Product_n,

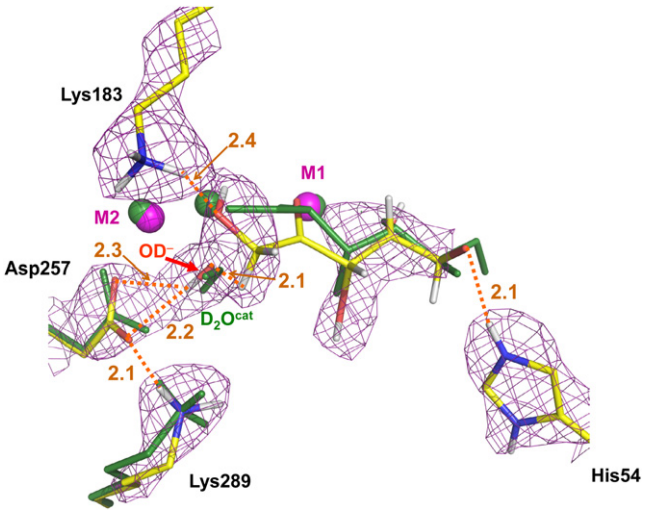

Figure 5. Linear Xylulose Product Binding in XI-Mg-Product_n and Comparison with XI-Ni-LinearSugar_n

Hydrogen bonds are shown as orange dashed lines and the O…D distances are in Å. Superposition of selected active-site residues and reactive water species in XI-Mg-Product_n (atom-type colored sticks and magenta spheres for Mg(II) cations) and XI-Ni-LinearSugar_n (dark green sticks and spheres). Neutron scattering density contoured at 1.2σ level is shown for XI-Mg-Product_n, in which His54, Lys183, and Lys289 are protonated and hydrogen-bonded to O5, O1, and Asp257, respectively. Linear perdeuterated xylulose and glucose superimpose well, except for the C2(O2)-C1(O1) portions of the molecules. The catalytic water (D_2O^{cat}) in XI-Ni-LinearSugar_n and deuteroxide (OD^-) generated from it during the isomerization reaction in XI-Mg-Product_n occupy the same position.

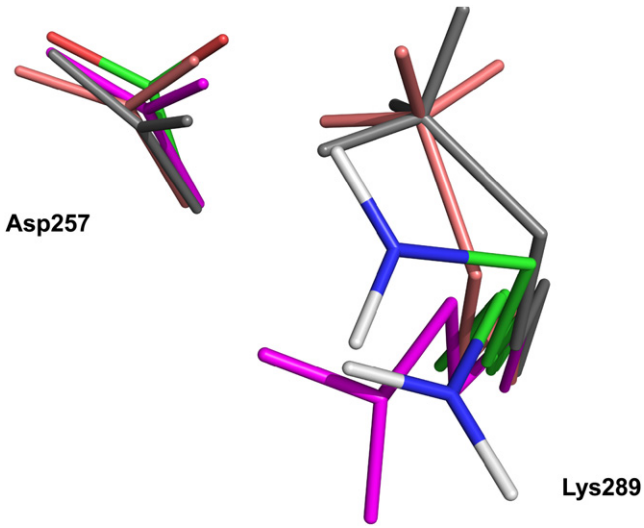

Figure 6. Lys289-Asp257 Diad

Superposition of Asp257-Lys289 diad in the four neutron structures: XI-Co_n's residues are colored by atom type (deuterium atoms are off-white); XI-Cd-CyclicSugar_n, magenta; XI-Ni-LinearSugar_n, salmon-red; XI-Mg-Product_n, gray.

C2 loses an H and C1 gains an H, the O1 aldehyde becomes protonated to a hydroxyl group, and O2 is deprotonated. In summary, H (as D) has been moved from D_2O^{cat}, C2, and O2, and has been moved to O1 and C1. M2 is disordered over two distinct positions in XI-Ni-LinearSugar_n in a way that suggests that the metal may move toward the aldehyde terminus of the linear sugar to bind to O1 and O2 during isomerization. This may, by the resulting charge distribution, affect how well the isomerization, that is the movement of H from C2 to C1, occurs. It would also appear that this disorder is induced by the sugar adopting the linear form after ring opening.

These observations do not support previous proposals for the isomerization reaction. In earlier hydride-shift mechanisms, proposed by Collyer et al. (1990) and Lee et al. (1990), there was no mention of the involvement of a catalytic water species bound to M2, while in later proposals (Fenn et al., 2004; Whitlow et al., 1991; Whitaker et al., 1995; Lavie et al., 1994), the presence of a catalytic hydroxide anion bound to M2 was necessary for the initiation of the hydride shift. In these different hydride shift proposals, this hydroxide ion would have to already be present in XI-Co_n before substrate binding, or it might be generated from the M2 bound catalytic water by the carboxylate group of Asp257 or Asp287 after the ring-opening step, and should therefore be present in XI-Ni-LinearSugar_n (which it is not). In either case, the hydroxide ion is believed to extract a proton from the sugar bound in its linear form, while M2 shifts to occupy a position where it can coordinate with both O1 and O2 to aid in the reaction. O1 is then thought to be protonated after C2-O2 has been transformed into a carbonyl group by the reactive M2-bound H_2O or by the protonated Asp257.

The important step in the isomerization mechanism is the movement of H from C2 to C1, and this appears to be aided by protonation of O1 and deprotonation of O2. We note that the results presented here do not rule out the possibility that H could be abstracted from C2 by the deprotonated D_2O^{cat} with D_2O^{cat} subsequently donating H to C1. An interesting aspect of these suggestions is that the ring opening acts as a trigger for the subsequent isomerization stage. The results presented here do not support H transfer from O2 to O1 by a native metal-activated hydroxide ion. One possibility is that the M2-bound catalytic water protonates the O1 aldehyde of the linear form of the sugar to produce a carbocation with the positive charge localized on C1. Perhaps the nickel metal present in XI-Ni-LinearSugar_n cannot sufficiently activate the catalytic water to donate its proton, whereas Mg^{2+}, Mn^{2+}, or Co^{2+} cations can. This is supported by the fact that the catalytic water is a hydroxyl ion in XI-Mg-Product_n. If O1 is indeed protonated in this fashion, then it might be expected that the O2 hydroxyl, coordinated to both M1 and M2, will become quite acidic and could be deprotonated by the nearest carboxylate, Asp287, which moves the proton into the bulk solvent through a network of water molecules. H transfer from C2 to C1 would be expected to occur after or at the same time as O2 deprotonation occurs (Figure 7).

Metal Coordination and Inhibition

The mean coordination distances for M1 do not change significantly over the four structures XI-Co_n, XI-Cd-CyclicSugar_n, XI-Ni-LinearSugar_n, and XI-Mg-Product_n. As shown in Figure S1 and Table S2, they are similar to the mean distances of 2.01 Å and 2.08(8) Å in the PDB determined at near atomic

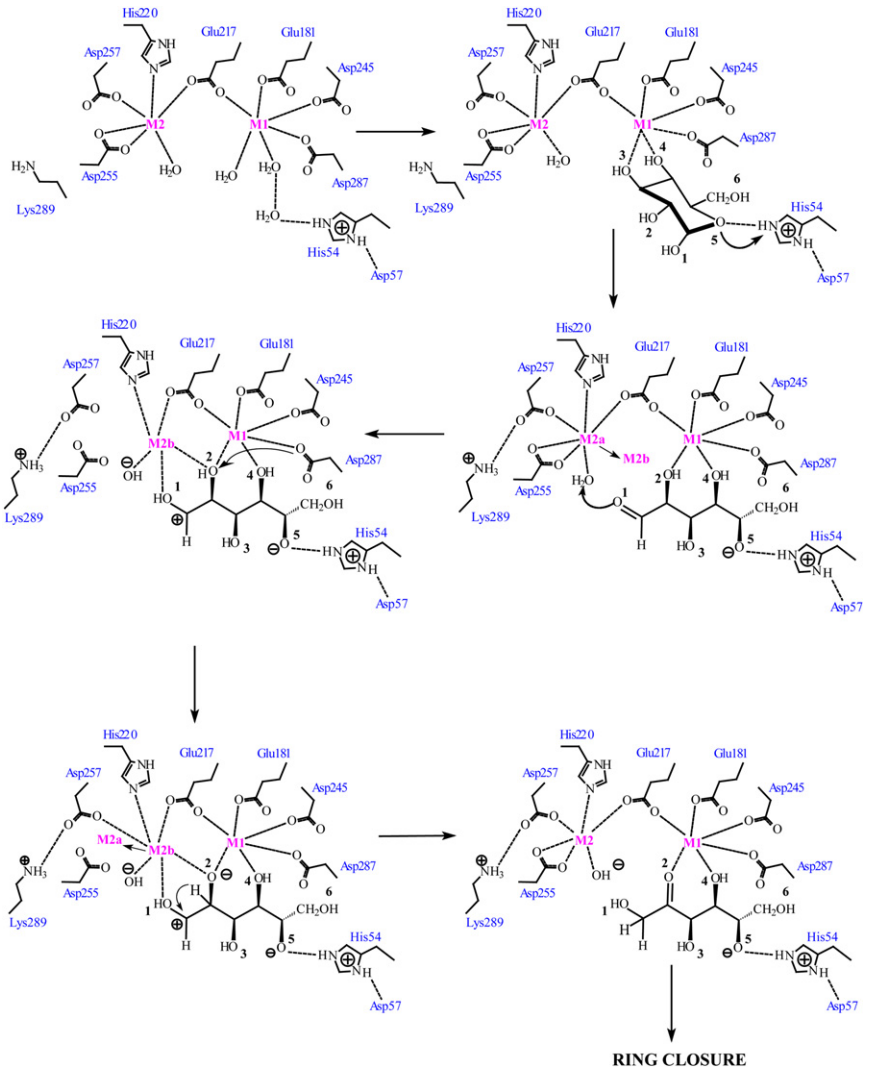

Figure 7. A Suggested Mechanism for Sugar Interconversion Reaction Catalyzed by XI

resolution for Co and Mg metals coordinating with monodentate carboxylates, respectively (Harding, 2006). M2, on the other hand, would appear to be more labile and mobile, and is found in two distinct positions, M2a and M2b, in the XI-Ni-LinearSugar_n complex. Although the mean coordination distances for M2 show greater variation from structure to structure, it is difficult to infer anything about changes in the strength of these interactions, because the metal cation is different in each complex.

Interestingly, the standard deviation associated with the mean coordination distance around both M1 and M2 in XI-Cd-CyclicSugar_n is relatively small compared with those for the other structures, indicating a more symmetric octahedral geometry. This geometry may better localize the metal and restrict its mobility. Cd^{2+} has an ionic radius of almost 1 Å, which is larger than the empirical threshold of 0.8 Å that has been observed for an active enzyme. Inhibition may be due to the increased ionic radius producing a softer electrostatic interaction with donors. However, it may also be due to a more restricted mobility caused by the relatively symmetric octahedral geometry.

Whereas Cd^{2+} inhibits ring opening, Ni^{2+} inhibits the next step: isomerization. The ionic radius of Ni^{2+} is less than 0.8 Å, and is similar to that of metal cations that promote enzyme activity. The inhibiting effect of Ni^{2+}, as well as Zn^{2+} and Cu^{2+}, on enzymatic reactions has previously been explained by their preference for nonoctahedral coordination geometries and their higher electron affinities compared with those of Mg^{2+} and Co^{2+} (Glusker, 1991; Vallee and Williams, 1968; Williams, 1970). In other words, Ni^{2+} is a softer acid than Co^{2+} or Mg^{2+}, preferring a more square planar coordination. Ni^{2+} may therefore be incapable of inducing the polarization of the catalytic water necessary to proceed with isomerization. Ni^{2+} at M2a in XI-Ni-LinearSugar_n is weakly bound to His220 and the catalytic water, and is better described as having square planar coordination geometry. At the M2b position, Ni^{2+} is five-coordinated, having a square pyramidal geometry with the O2 hydroxyl of the linear glucose at the apex of the square pyramid. Interestingly, and perhaps importantly for the isomerization reaction to proceed, Ni^{2+} at M2b makes good coordination bonds with His220 of 2.0 Å and with the catalytic water of 1.9 Å (Figure S1 and Table S2). It has been shown that mutations of His220 result in an inactive enzyme (Cha et al., 1994).

New Insights into the Overall Reaction Mechanism

The results presented here do not support some aspects of previous proposals for the reaction mechanism, but rather lead to new suggestions as to how changes might take place over the course of the reaction, which we summarize here and in Figure 7. The new findings are: (1) different arrangements of ordered water molecules appear to function as templates for binding the cyclic and linear substrates; (2) Lys289 is neutral before ring opening and is protonated after; (3) Lys289 is rotated away from Asp257 before ring opening but donates H in a hydrogen bond to Asp257 after; (4) O1 is protonated before ring opening but is deprotonated after, accepting H in a hydrogen bond from Lys183; (5) O5 is deprotonated after ring opening; (6) His54 remains doubly protonated on its ring N's throughout; (7) the catalytic metal-bound solvent molecule is a water molecule before isomerization and an hydroxyl ion after; and (8) the catalytic metal (M2) occupies two sites after ring-opening and before isomerization.

We interpret these new findings mechanistically as follows. Results (2) and (4) indicate that H moves to Lys289 and that H moves from O1 during ring opening. There is no evidence that Lys289 abstracts H from O1, but it would be consistent with these results. Results (5) and (6) indicate that the His54…Asp57 pair does not permanently donate a proton to O5 during ring opening. There is no evidence that His54 transiently gives its extra proton to O5 and then reclaims it after the C1-O5 endo-cyclic bond is broken, but it is a possibility that would be consistent with these results. From result (4), it is clear that after ring opening O1 swings toward Lys183, displacing W4 to accept a proton in a hydrogen bond and toward M1 preparing the aldehyde group for the isomerization. Result (8) indicates that the opening of the sugar into its linear form causes disorder of the catalytic metal cation at M2. One possible explanation for this disorder is that the metal cation can move from its M2a position to the M2b site and toward the aldehyde terminus to bind to O1 and O2. Result (7) indicates that H is moved from D_2O^{cat} during isomerization. There is no direct evidence to indicate which atom this H is given to. However, we note that O1 is deprotonated before isomerization and protonated after. It would therefore be consistent with these results if the M2-bound catalytic water protonates the O1 aldehyde of the linear form of the sugar to produce a carbocation with the positive charge localized on C1. If O1 is indeed protonated in this fashion, then it might be expected that the O2 hydroxyl, coordinated to both M1 and M2b, will become quite acidic and could be deprotonated by the nearest carboxylate of Asp287, which moves the proton into the bulk solvent through a network of water molecules. The results also clearly indicate that C2 loses H and C1 gains H during isomerization. However, there is no direct evidence for the exact mechanism for this movement.

Several aspects of the mechanism remain to be unambiguously determined. In particular: the exact roles of Lys289 protonation and O1 deprotonation during ring opening and their relationship to each other; whether the catalytic metal cation is indeed mobile or simply disordered; whether or not D_2O^{cat} directly protonates O1; and any further role of the deprotonated D_2O^{cat} during isomerization. The exact mechanism for the movement of H from C2 to C1 also requires further investigation; it is not clear whether H from C2 is given to C1 as a hydride anion (H^-) in a simple hydride shift (perhaps aided by the close proximity of the metal in position M2b), as a hydrogen ion (H^+) through hyperconjugation in which the C1-C2 bond gains the double bond character while the positive charge on C1 is shifted to the H on C2 weakening this C2-H bond, or by abstraction from C2 by the deprotonated D_2O^{cat} with D_2O^{cat} subsequently donating H to C1. Despite these remaining questions, our hope is that the results of our neutron-diffraction studies will not only contribute toward an understanding of the mechanism of this much-studied enzyme, but might also prove useful in engineering efforts to improve its use and performance.

EXPERIMENTAL PROCEDURES

Sample Preparation

Sample preparation for XI-Co_n and XI-Mg-Product_n has been previously described (Katz et al., 2006; Hanson et al., 2004) To obtain complexes XI-Mg/Ni, XI-Ni, XI-Cd, XI-Cd-CyclicSugar, and XI-Ni-LinearSugar, XI (MW = 172 kDa) was purchased from Hampton Research Corp. (Aliso Viejo, CA). Each batch was dialyzed three times against 100mM TRIS buffer (pH = 8.0) containing 10mM EDTA to remove all intrinsic metal and then twice against 100mM HEPES (pH = 7.7). The resulting *apo*-enzyme was concentrated to ~80 mg/ml. Crystallization trials started with a determination of the phase diagram with an Oryx8 crystallization robot (Douglas Instruments Ltd, East Garston, Hungerford, Berkshire, UK) using microbatch crystallization under paraffin oil. Best conditions for growing large crystals of XI-*apo* were found to be a 40 mg/ml enzyme, which corresponds to ~1mM monomeric XI, mixed with 30% saturated ammonium sulfate buffered to a pH of 7.7. Crystals suitable for neutron and X-ray diffraction experiments were grown at 17°C in nine well-siliconized glass plates supplied by Hampton Research, using batch crystallization, a volume of 500 μl, and no oil. Crystals as large as 50 mm^3 grew within 3-4 weeks. Binary complexes of XI with metal cofactors were prepared in the following way. A crystallization drop containing an XI-*apo* crystal was injected with an aqueous solution of the desired metal salt so that the metal ion concentration increased stepwise to 5 mM over a period of five days, resulting in a 2.5-fold metal-to-enzyme concentration. Injections were made once a day in 1mM increments until the final metal concentration was achieved. Ternary complexes with substrate were prepared from the binary complexes by injecting the drop with perdeuterated glucose (D-[d_{12}]-glucose, 97% D, Sigma-Aldrich), stepwise, reaching a final sugar concentration of 400-500 mM. Injections of D-[d12]-glucose were made once a day in 100mM increments until the final sugar concentration was achieved. The final concentration corresponds to 2 to 2.5 times the K_M value of XI for glucose.

Small crystals for X-ray crystallographic studies were mounted in thin-walled quartz capillaries with a mother liquor plug, and then sealed with wax. Larger crystals for neutron crystallographic studies were sealed in quartz tubes crafted into hour-glass shapes, and sealed with wax. The lower part of each tube was filled with 400–500 μl of $(ND_4)_2SO_4$/HEPES solution made with 100% D_2O. This solution was replaced every couple of weeks over a period of several months to ensure the exchange of all labile and accessible H atoms by D.

X-ray Crystallography

X-ray crystallographic data sets were collected from a number of XI binary and ternary complexes, to search for combinations of metal cofactors and substrates that bound in the desired forms and to screen for crystallization conditions that produced the best diffraction data quality. All data sets were collected at room temperature on a Rigaku FR-E with R-Axis VI++ detector. Diffraction data were integrated and scaled using the CrystalClear/d*TREK software (Pflugrath, 1999), and the structures were refined using SHELX (Sheldrick and Schneider, 1997). The X-ray structures determined from XI binary complexes with the different metal cations Ni and Cd but no substrate, XI-Ni_x (PDB ID: 3KBV) and XI-Cd_x (PDB ID: 3KBS), were used to assess the effect of using metal cations with different radii on the geometry of the active site. X-ray structures were also determined from representative crystals before and after H/D exchange to ensure that this process did not significantly change the structure of the active site. When using joint X-ray and neutron (XN) strategies for structure refinement, the process is greatly simplified if the X-ray and neutron data have been collected from isomorphous crystals. In order to ensure this, the X-ray data were collected from crystals that had been taken from the same crystallization drops that provided the larger crystals for neutron data sets and were exchanged with D_2O in a similar way as was done for neutron studies. These data were used to determine the structures of XI-Cd-CyclicSugar_x and XI-Ni-LinearSugar_x, and then in joint refinements with neutron data to determine the structures of XI-Cd-CyclicSugar_n and XI-Ni-LinearSugar_n. A summary of the crystallographic data is given in Table 2 and Table S1.

Neutron Crystallography

Time-of-flight Laue neutron crystallographic data were collected to 1.8 Å resolution from XI-Ni-LinearSugar_n at room temperature on the PCS at Los Alamos National Laboratory (Langan et al., 2004) using previously described techniques. The data were measured with a version of *d*TREK* (Pflugrath, 1999) adapted for time-of-flight geometry (Langan and Greene, 2004), wavelength normalized using *LAUENORM* (Helliwell et al., 1989), and then merged with *SCALA* from the *CCP4i*46 (Weiss, 2001; Potterton et al., 2003) suite of programs. Monochromatic neutron data were collected from XI-Cd-CyclicSugar_n to 1.8 Å resolution at room temperature on D19 at the Institut Laue

Langevin (ILL), using ω step-scans (0.07° with an exposure time of 60 to 100 s per step) and a wavelength of 2.422 Å. The data were processed with the ILL program RETREAT (Wilkinson et al., 1998), corrected for effective absorption, and then merged with *SCALA* from the *CCP4i* (Weiss, 2001; Potterton et al., 2003) suite of programs. A summary of the experimental and refinement statistics is given in Table 1.

Joint XN Structure Determination

The joint X-ray and neutron (XN) structures of XI-*apo*_n, XI-Cd-CyclicSugar_n and XI-Ni-LinearSugar_n were determined using *nCNS* (Adams et al., 2009). After rigid body refinement, there followed several macrocycles of positional, atomic displacement parameter, and occupancy refinement, followed by water building. The structures were then checked and side-chain conformations altered, if necessary, based on the F_O-F_C neutron scattering density map. The $2F_O$-F_C and F_O-F_C neutron scattering density maps were then inspected to determine the orientation of hydroxyl groups in amino acid side chains and also the protonation states of His and Lys residues. The protonation states of some disordered side chains could not be directly obtained.

All water molecules were refined as D_2O. Water oxygen atoms were initially positioned according to their electron density peaks, and remained relatively unchanged. The orientations of water molecules were examined and altered based on the potential hydrogen-bond donors and acceptors. Some waters were eliminated from the refinement when no $2F_O$-F_C neutron scattering density could be observed, accounting for the difference in the number of reported solvent molecules between identical X-ray and neutron structures. The level of H/D exchange at labile positions on the enzyme was also refined. All labile H positions were modeled as D and then the occupancy of D was allowed to refine within the range of −0.56 to 1.00 (the scattering length of H is −0.56 times the scattering length of D). Before depositing the final structures to the PDB, a script was run that converts a record for the coordinate of a labile D atom into two records corresponding to an H and a D atom partially occupying the same coordinate, both with positive partial occupancies that add up to unity. The refinement statistics are represented in Table 1.

ACCESSION NUMBERS

Coordinates have been deposited in the PDB with accession numbers: 3KBM, 3KBN, 3KBS, 3KBV, 3KBW, 3KCL, 3KCO.

SUPPLEMENTAL INFORMATION

Supplemental Information includes two tables and two figures and can be found with this article online at doi:10.1016/j.str.2010.03.011.

ACKNOWLEDGMENTS

The PCS is funded by the Office of Biological and Environmental Research of the Department of Energy. The PCS is located at the Lujan Center at Los Alamos Neutron Science Center, funded by the DOE Office of Basic Energy Sciences. M.M. and P.L. were partly supported by an NIH-NIGMS funded consortium (1R01GM071939-01) between LANL and LNBL to develop computational tools for neutron protein crystallography. A.Y.K. was partly supported by LANL, LDRD grant (20080789PRD3). A.Y.K. and P.L. were partly supported by a LANL, LDRD grant (20070131ER), JPG CA10925 and Fox Chase CA06927, both from NIH. B.L.H. is supported by NSF 446218. V.T.F. and S.A.M. acknowledge support from EPSRC under grants GR/R47950/01, GR/R99393/01, EP/C015452/1. The new D19 diffractometer was built as part of a collaboration between Durham University, Keele University, Bath University, and ILL. We gratefully acknowledge the help of John Archer, John Allibon, and the efforts of the ILL detector group.

Received: October 22, 2009
Revised: January 11, 2010
Accepted: March 8, 2010
Published: June 8, 2010

REFERENCES

Adams, P.D., Mustyakimov, M., Afonine, P.V., and Langan, P. (2009). Generalized X-ray and neutron crystallographic analysis: more accurate and complete structures for biological macromolecules. Acta Crystallogr. D *65*, 567–573.

Allen, K.N., Lavie, A., Glasfeld, A., Tanada, T.N., Gerrity, D.P., Carlson, S.C., Farber, G.K., Petsko, G.A., and Ringe, D. (1994a). Role of the divalent metal ion in sugar binding, ring opening, and isomerization by D-xylose isomerase: Replacement of a catalytic metal by an amino acid. Biochemistry *33*, 1488–1494.

Allen, K.N., Lavie, A., Glasfeld, A., Petsko, G.A., and Ringe, D. (1994b). Isotopic exchange plus substrate and inhibition kinetics of D-xylose isomerase do not support a proton-transfer mechanism. Biochemistry *33*, 1481–1487.

Asboth, B., and Naray-Szabo, G. (2000). Mechanism of action of D-xylose isomerase. Curr. Protein Pept. Sci. *1*, 237–254.

Bhosale, S.H., Rao, M.B., and Deshpande, V.V. (1996). Molecular and industrial aspects of glucose Isomerase. Microbiol. Rev. *60*, 280–300.

Blakeley, M.P., Langan, P., Niiumra, N., and Podjarny, A. (2008). Neutron crystallography: opportunities, challenges, and limitations. Curr. Opin. Struct. Biol. *18*, 593–600.

Blow, D.M., Collyer, C.A., Goldberg, J.D., and Smart, O.S. (1992). Structure and mechanism of D-xylose isomerase. Faraday Discuss. *93*, 67–73.

Bock, K., Meldal, M., Meyer, B., and Wiebe, L. (1983). Isomerization of D-glucose with glucose isomerase. A mechanistic study. Acta Chem. Scand. B *37*, 101–108.

Callens, M., Kersters-Hilderson, H., van Opstal, O., and De Bruyne, C.K. (1986). Catalytic properties of D-xylose isomerase from *Streptomyces violaceoruber*. Enzyme and Microbial Technology *8*, 696–700.

Carrell, H.L., Glusker, J., Burger, P.V., Manfre, F., Tritsch, D., and Biellmann, J.F. (1989). X-ray analysis of D-xylose isomerase at 1.9 Å: Native enzyme in complex with substrate and with a mechanism-designed inactivator. Proc. Natl. Acad. Sci. USA *86*, 4440–4444.

Cha, J., Cho, Y., Whitaker, R.D., Carrell, H.L., Glusker, J.P., Karplus, P.A., and Batt, C.A. (1994). Perturbing the metal site in D-xylose isomerase. effect of mutations of His220 on enzyme activity. J. Biol. Chem. *269*, 2687–2694.

Chandrakant, P., and Bisaria, V.S. (2000a). Application of a compatible xylose isomerase in simultaneous bioconversion of glucose and xylose to ethanol. Biotechnolongy and Bioprocess Engineering *5*, 32–39.

Chandrakant, P., and Bisaria, V.S. (2000b). Simultaneous bioconversion of glucose and xylose to ethanol by *Saccharomyces cerevisiae* in the presence of xylose isomerase. Appl. Microbiol. Biotechnol. *53*, 301–309.

Chen, W.-P. (1980). Glucose isomerase (a review). Process Biochem. *15*, 36–41.

Collyer, C.A., Henrick, K., and Blow, D.M. (1990). Mechanism for aldose-ketose interconversion by D-xylose isomerase involving ring opening followed by a 1,2-hydride shift. J. Mol. Biol. *212*, 211–235.

Collyer, C.A., Goldberg, J.D., Viehmann, H., Blow, D.M., Ramsden, N.G., Fleet, G.W.J., Montgomery, F.J., and Grice, P. (1992). Anomeric specificity of D-xylose isomerase. Biochemistry *31*, 12211–12218.

Danno, G.-I. (1970). Studies on D-glucose-isomerizing enzyme from *Bacillus coagulans*, strain HN-68. Part V. Comparative study on the three activities of D-glucose, D-xylose, and D-ribose isomerization of the crystalline enzyme. Agric. Biol. Chem. *34*, 1805–1814.

Farber, G.K., Glasfeld, A., Tiraby, G., Ringe, D., and Petsko, G.A. (1989). Crystallographic studies of the mechanism of xylose isomerase. Biochemistry *28*, 7289–7297.

Fenn, T.D., Ringe, D., and Petsko, G.A. (2004). Xylose isomerase in substrate and inhibitor Michaelis states: atomic resolution studies of a metal-mediated hydride shift. Biochemistry *43*, 6464–6474.

Gaikwad, S.M., More, M.W., Vartak, H.G., and Deshpande, V.V. (1988). Evidence for the essential histidine residue at the active site of glucose/xylose isomerase from streptomyces. Biochem. Biophys. Res. Commun. *155*, 270–277.

 ©2010 Elsevier Ltd All rights reserved

Glusker, J.P. (1991). Structural aspects of metal liganding in functional groups in proteins. Adv. Protein Chem. *42*, 1–76.

Hanson, B.L., Langan, P., Katz, A.K., Li, X., Harp, J.M., Glusker, J.P., Schoenborn, B.P., and Bunick, G.J. (2004). A preliminary time-of-flight neutron diffraction study of *Streptomyces rubiginosus* D-xylose isomerase. Acta Crystallogr. D Biol. Crystallogr. *60*, 241–249.

Harding, M.M. (2001). Geometry of metal-ligand interactions in proteins. Acta Crystallogr. D Biol. Crystallogr. *57*, 401–411.

Harding, M.M. (2006). Small revision to predicted distances around metal sites in proteins. Acta Crystallogr. D Biol. Crystallogr. *62*, 678–682.

Hartley, B.S., Hanlon, N., Jackson, R.J., and Rangarajan, M. (2000). Glucose isomerase: Insights into protein engineering for increased thermostability. Biochim. Biophys. Acta *1543*, 294–335.

Helliwell, J.R., Habash, J., Cruickshank, D.W.J., Harding, M.M., Greenhough, T.J., Campbell, J.W., Clifton, I.J., Elder, M., Machin, P.A., Papiz, M.Z., and Zurek, S. (1989). The recording and analysis of synchrotron X-radiation Laue diffraction photographs. J. Appl. Cryst. *22*, 483–497.

Henrick, K., Collyer, C.A., and Blow, D.M. (1989). Structures of D-xylose isomerase from *Arthrobacter* strain B3728 containing the inhibitors xylitol and D-sorbitol at 2.5 Å and 2.3 Å resolution respectively. J. Mol. Biol. *208*, 129–157.

Jenkins, J., Janin, J., Rey, F., Chiadmi, M., van Tilbeurgh, H., Lasters, I., De Maeyer, M., van Belle, D., Wodak, S.J., Lauwereys, M., et al. (1992). Protein engineering of xylose (glucose) isomerase from *Actinoplanes missouriensis*. 1. Crystallography and site-directed mutagenesis of metal binding site. Biochemistry *31*, 5449–5458.

Katz, A.K., Li, X., Carrell, H.L., Hanson, B.L., Langan, P., Coates, L., Schoenborn, B.P., Glusker, J.P., and Bunick, G.J. (2006). Locating active-site hydrogen atoms in D-xylose isomerase. Time-of-flight neutron diffraction. Proc. Natl. Acad. Sci. USA *103*, 8342–8347.

Kossiakoff, A.A., and Spencer, S.A. (1980). Neutron diffraction identifies His 57 as the catalytic base in trypsin. Nature *288*, 414–416.

Kovalevsky, A.Y., Katz, A.K., Carrell, H.L., Hanson, L., Mustyakimov, M., Fisher, S.Z., Coates, L., Schoenborn, B.P., Bunick, G.J., Glusker, J.P., and Langan, P. (2008). Hydrogen location in stages of an enzyme-catalyzed reaction: time-of-flight neutron structure of D-xylose isomerase with bound xylulose. Biochemistry *47*, 7595–7597.

Langan, P., and Greene, G. (2004). Protein crystallography with spallation neutrons: collecting and processing wavelength-resolved Laue protein data. J. Appl. Cryst. *37*, 253–257.

Langan, P., Greene, G., and Schoenborn, B.P. (2004). Protein crystallography with spallation neutrons: the user facility at Los Alamos Neutron Science Center. J. Appl. Cryst. *37*, 24–31.

Lavie, A., Allen, K.N., Petsko, G.A., and Ringe, D. (1994). X-ray crystallographic structures of D-xylose isomerase-substrate complexes position the substrate and provide evidence for metal movement during catalysis. Biochemistry *33*, 5469–5480.

Lee, C.Y., Bagdasarian, M., Meng, M., and Zeikus, J.G. (1990). Catalytic Mechanism of Xylose (Glucose) Isomerase from *Clostridium thermosulfurogenes*. J. Biol. Chem. *265*, 19082–19090.

Pflugrath, J.W. (1999). The finer things in X-ray diffraction data collection. Acta Crystallogr. D Biol Crystallogr. *55*, 1718–1725.

Potterton, E., Briggs, P., Turkenburg, M., and Dodson, E. (2003). A graphical user interface to the *CCP*4 program suite. Acta Crystallogr. D Biol Crystallogr. *59*, 1131–1137.

Rose, I.A., O'Connell, E.L., and Mortlock, R.P. (1969). Biochim. Biophys. Acta *178*, 376–379.

Schray, K.J., and Rose, I.A. (1971). Anomeric specificity of two pentose isomerases. Biochemistry *10*, 1058–1062.

Sears, V.F. (1992). Neutron scattering lengths and cross sections. Neutron News *3*, 26–37.

Sheldrick, G.M., and Schneider, T.R. (1997). High resolution refinement. Methods Enzymol. *277*, 319–343.

Suekane, M., Tamura, M., and Tomimura, C. (1978). Physicochemical and enzymatic properties of purified glucose isomerase from *Streptomyces olivochromogenes* and *Bacillus stearothermophilus*. Agric. Biol. Chem. *42*, 909–917.

Vallee, B.L., and Williams, R.J.P. (1968). Metalloenzymes: the entatic nature of their active sites. Proc. Natl. Acad. Sci. USA *59*, 498–505.

Weiss, M.S. (2001). Global indicators of X-ray data quality. J. Appl. Cryst. *34*, 130–135.

Whitaker, R.D., Cho, Y., Cha, J., Carrell, H.L., Glusker, J.P., Karplus, P.A., and Batt, C.A. (1995). Probing the roles of active site residues in D-xylose isomerase. J. Biol. Chem. *270*, 22895–22906.

Whitlow, M., Howard, A.J., Finzel, B.C., Poulos, T.L., Winborne, E., and Gilliland, G.L. (1991). A metal-mediated hydride shift mechanism for xylose isomerase based on the 1.6 Å *Streptomyces ribiginosus* structures with xylitol and D-xylose. Prot. Struct. Funct. Genet. *9*, 153–173.

Wilkinson, C., Khamis, H.W., Stansfield, R.F.D., and McIntyre, G.J. (1998). Integration of single-crystal reflections using area multidetectors. J. Appl. Cryst. *21*, 471–478.

Williams, R.J.P. (1970). The biochemistry of sodium, potassium, magnesium, and calcium. Q. Rev. Chem. Soc. *24*, 331–365.